HAL
open science

Extreme precipitation in the tropics is closely associated with long-lived convective systems

Rémy Roca, Thomas Fiolleau

To cite this version:

Rémy Roca, Thomas Fiolleau. Extreme precipitation in the tropics is closely associated with long-lived convective systems. Communications Earth & Environment, 2020, 1 (1), 10.1038/s43247-020-00015-4 . hal-03035461

HAL Id: hal-03035461

https://cnrs.hal.science/hal-03035461v1

Submitted on 2 Dec 2020

HAL is a multi-disciplinary open access archive for the deposit and dissemination of scientific research documents, whether they are published or not. The documents may come from teaching and research institutions in France or abroad, or from public or private research centers.

L'archive ouverte pluridisciplinaire **HAL**, est destinée au dépôt et à la diffusion de documents scientifiques de niveau recherche, publiés ou non, émanant des établissements d'enseignement et de recherche français ou étrangers, des laboratoires publics ou privés.

COMMUNICATIONS EARTH&ENVIRONMENT

ARTICLE

https://doi.org/10.1038/s43247-020-00015-4 OPEN

Extreme precipitation in the tropics is closely associated with long-lived convective systems

Rémy Roca [1✉] & Thomas Fiolleau [1]

Water and energy cycles are linked to global warming through the water vapor feedback and heavy precipitation events are expected to intensify as the climate warms. For the mid-latitudes, extreme precipitation theory has been successful in explaining the observations, however, studies of responses in the tropics have diverged. Here we present an analysis of satellite-derived observations of daily accumulated precipitation and of the characteristics of convective systems throughout the tropics to investigate the relationship between the organization of mesoscale convective systems and extreme precipitation in the tropics. We find that 40% of the days with more than 250 mm precipitation over land are associated with convective systems that last more than 24 hours, although those systems only represent 5% of mesoscale convective systems overall. We conclude that long-lived mesoscale convective systems that are well organized contribute disproportionally to extreme tropical precipitation.

[1] Laboratoire d'Études en Géophysique et Océanographie Spatiales (Université de Toulouse III, CNRS, CNES, IRD), Toulouse, France. ✉email: remy.roca@legos.obs-mip.fr

Water and energy cycles are intimately linked to global warming through the water vapor feedback[1]. Specifically, as temperature increases, the concentration of water vapor in the atmosphere increases[2]. This extra amount of water vapor results in an increase in global precipitation at a rate constrained by the global energy budget[3] and is also thought to increase the intensity of heavy precipitation events[4]. The rate of increase of extreme rainfall with surface temperature can be derived from an elegant quantitative theory based on vertical dynamics, cloud/rain microphysics, and thermodynamics of the atmospheric column[5]. This theory has had great success in explaining the observational record as well as high-resolution climate model simulations and predictions, in mid-latitudes environment[6] but is actively discussed in the case of the tropics[7–9]. In the tropics, conventional observation-based studies and idealized cloud resolving simulations indeed span a large diversity of responses to warming prompting for a deeper understanding of how organization of convection can lead to extreme precipitation[10].

Mesoscale convective systems (MCS) have long been recognized as a major source of precipitation in the tropics[11–13]. MCS thus appear as natural candidates for being a prominent contributor to extreme precipitation too; however, a robust quantification of this relationship has remained elusive. Indeed, even if the organized nature of deep convection in the tropics is well recognized[14], its objective characterization is complicated. In addition, heavy precipitation depends on many other factors, linked to the environment and or linked to the MCS's internal dynamics and microphysics. These factors are all related to the life cycle of the deep convective systems[11,15].

Qualitative features of deep convection within its environment are frequently used as an indicator of organization. Convective self aggregation[16] put the emphasis on spatial organization. Observations show that the strength of tropical precipitation extremes can be modulated by aggregation[17]. Cloud resolving simulations indicate that aggregated vs. non-aggregated states seem to only influence extreme rainfall intensity at daily but not at instantaneous scale[18]. Statistically determined weather-states analysis based on cloud top properties from the International Satellite Cloud Climatology Project (ISCCP) have also been correlated with tropical precipitation[19]. The weather state #1, associated with organized convection at mesoscale, including long-lived systems, is shown to relate well with recent trends in tropical precipitation[20] as well as with extreme precipitation distribution[21].

Quantitative investigations, on the other hand, opt for using the morphological features of storms to describe their degree of organization[22]. Analysis of snapshots of precipitation from space-borne radars indicates that large precipitation features, while rare contribute significantly to total precipitation[23]. Nevertheless, over tropical oceans, the relationship between snapshots of extremely tall convective systems and the systems with extreme surface rainfall is weak but the heaviest rainfall events appear more organized than the other[24]. Even though precipitation features based analysis is informative in its own right, it often does not provide explicitly insight into the life-cycle of the storm. Regional studies emphasize strong relationship between the size and extreme precipitation[25,26] as well as duration of storms and environmental wind shear[27,28]. Idealized simulations of static squall lines, a well-known example of highly organized deep convection, shows CC-like response at instantaneous scale[29], while more realistic propagating squall lines simulations appear to support super-CC rate[30]. In the latter case, simulations at daily scale suggest that there is no clear relationship between extreme precipitation and intensity of the warming.

The characteristics of extreme precipitating storms in the tropics remain mostly qualitative, lacking in key aspects of the life cycle of organized convection. The more recent generation of satellite-based gridded precipitation products[31] exhibits a robust thermodynamic scaling with surface temperature over tropical land, at a rate of change consistent with the theory[9]. This consistency suggests that these precipitation estimates are well-suited to document the complex, yet remarkably organized, nature of extreme precipitation in the tropics[32]. We therefore investigate here the statistical relationship between morphology of convective systems and extreme precipitation by pooling data from all over the tropics. We quantify this relationship using recent satellite-derived and well-curated databases of both daily accumulated precipitation and convective systems characteristics. We focus on the duration of the system as a physically sound and key metric to quantify convective organization. Despite being infrequent, long-lasting convective systems do have an overwhelming contribution to total tropical precipitation amount[13]. We show here that these infrequent, long-lasting systems are also largely responsible for the tropical extreme precipitation.

Results

Distribution of tropical precipitation from satellite observations. A sub-ensemble of satellite-based products is used to characterize precipitation distribution across the whole tropical region (See Methods). The sub-ensemble focuses on constellation based products which have been shown robust to be well-suited and reliable to document the extreme precipitation[9]. For land and ocean, the probability of exceedance, defined as the number of grid boxes above a given threshold of precipitation intensity divided by the total number of grid boxes, gradually decreases with threshold (Fig. 1). Above 20 mm/d and up to the full range of precipitation rate considered here, the oceanic probability is

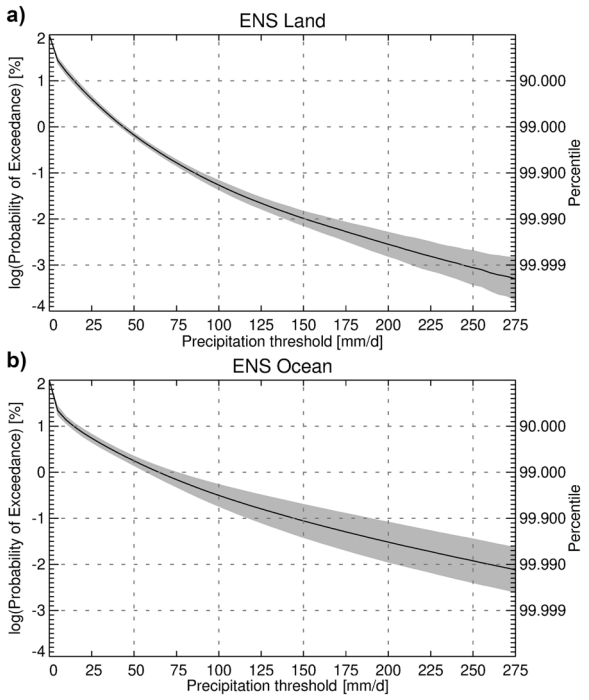

Fig. 1 The probability of exceedance of precipitation threshold shows the rarity of the very intense precipitation conditions. a Over land and **b** over ocean. The black curve corresponds to the ensemble mean probability in %. The gray shading area corresponds to the spread within the precipitation products ensemble based on one relative standard deviation (see "Methods").

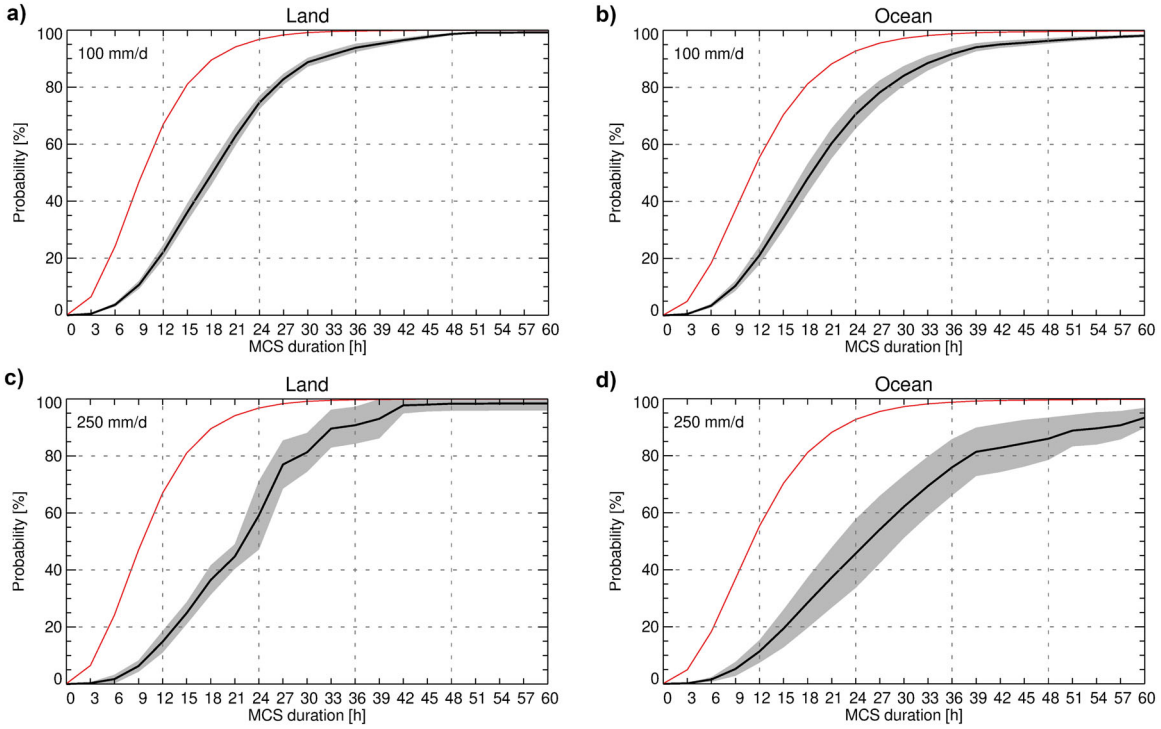

Fig. 2 The joint precipitation-MCS distribution reveals the role of the long-lived systems to the extreme precipitation. The ensemble mean probability of precipitation occurrence exceeding a threshold as a function of MCS duration. The gray shading corresponds to ± one standard deviation of the precipitation products ensemble. The red curve is the cumulated distribution function of the MCS occurrence for all precipitation above 0 mm/d. **a** For a threshold of 100 mm/d over land and (**b**) of 100 mm/d over ocean (**c**) of 250 mm/d over land and (**d**) of 250 mm/d over ocean.

systematically higher than over land. The spread in the sub-ensemble is larger over ocean than land probably owing to the common usage of rain gauges by the products over land. Note that the 99.9th percentile of the distribution corresponds roughly to 85 mm/d and 150 mm/d over land and ocean, respectively. Here we extend our analysis to a much higher threshold of 250 mm/d. This regime will be referred to in the following as "extreme" extreme precipitation.

Distribution of mesoscale convective systems in the tropics. Tropical convective systems span a wide range of spatial scales from 10 to 1000 km and duration from a few hours to a few days. The morphology of cold cloud clusters, identified from geostationary satellite observations in the thermal infrared band (TOOCAN algorithm[33]), is used here as a marker of the organization of mesoscale deep convection. In particular, the systems' duration is an integral of the complex interplay of an ensemble of factors, ranging from internal mesoscale dynamics, cloud microphysics, and the interaction between deep convection and stratiform precipitation with the large scale environment[11]. Moreover, duration is strongly correlated with other morphological attributes (maximum cluster extension, propagation, etc…) over the whole tropics[22]. The processes responsible for the short or long duration of the systems are also very contrasted[34]. Overall, duration appears as a physically sound metric to quantity mesoscale convective organization.

The distribution of occurrence of these MCS is highly skewed towards shorter systems that are expectedly more frequent than long-lasting ones (Fig. 2, red curves). Over the continents, 60% of the population of MCS lasts <12 h, and 95% lasts <24 h. In contrast, systems on an average last longer over the oceans than over land; correspondingly, systems with duration up to 24 h only contribute to 90% of the MCS population. We also find that very long-lasting systems appear relatively rare over both tropical land and ocean, which is in agreement with previous studies[11,22,35,36].

Joint analysis of the precipitation and mesoscale convective systems distributions. Nearly 93% of total tropical rainfall is associated with MCS that occur relatively more frequently over land (~70%) than over ocean (~40%) (Table S2). Note that not all precipitation grid boxes are associated with cold cloudiness and MCS. The analysis of the probability of exceedance for the non-MCS precipitation grid boxes (green curve in Fig. S2) further indicates that while value up to 100 mm/d can be found in these cases, their probability of exceedance is 2 to 3 orders of magnitude smaller than for the all precipitation grid boxes cases and does not impact the results shown next.

For high thresholds (100 m/d or more) over land, we find that systems lasting more than 12 h represent nearly 80% of the probability of extreme rain accumulation; however, they correspond to ~30% of the MCS population (Fig. 2). Systems lasting more than 24 h still represent 25% of the extreme precipitation cases while accounting for <5% of the population. These contributions increase as more intense precipitation values are used (Fig. S4 for 150 and 200 mm/d). For daily precipitation exceeding 250 mm/d over land, systems lasting more than 24 h accounts for 40% of the extreme precipitation cases while corresponding <5% of the MCS distribution. Over the ocean, the situation is even more remarkable, with more than 50% of the heavy rain days being related to systems lasting more than 24 h. Even though the spread of the precipitation ensemble increases with precipitation intensity, it nevertheless remains small in comparison to the threshold. This is indicative of the robustness of the present findings to the selection of the precipitation observational product. This result suggests that a small category of rare storms contributes as much to the occurrence of extreme precipitation as the rest of the tropical storms. Thus, the systems

lasting more than 12 h, that are known to account for around 75% of tropical rainfall[13], also appear to control the distribution of extreme "extreme" precipitation over the entire tropics.

Summary and discussions

The relationship between extreme daily precipitation and the morphology of MCS is investigated over tropical land and ocean thanks to a joint analysis of an ensemble of satellite-based precipitation products and of satellite observations of cold cloudiness. The pooling of data over the whole tropics reveals a clear picture where the probability of experiencing a heavy rain event is shown to be a steep function of the cumulated distribution of the duration of the MCS. In short, "extreme" extreme precipitation events are primarily contributed by a specific category of convective systems, namely the very long-lived systems. These findings are robust and invariant to the selection of precipitation product as indicated by the small ensemble spread.

The identification of very well organized, long-lived systems as a key element of tropical water cycle offers an avenue to better understand the role of organized convection at mesoscale in extreme precipitation[10]. Designing long-lived systems dedicated cloud-resolving experiments, so far missing, would help in providing clarity on the thermodynamic, dynamical, and microphysical processes at play in extreme precipitation cases. The ready availability of tracking algorithms on model simulations[37] permits the use of the proposed duration metrics in model-based investigations.

From a broader perspective, the understanding of evolution of extreme precipitation under climate change is directly related to the evolution of long-lived MCS in a warmer world, assuming that the relationships extracted in this study hold for the future. Our results strengthen the notion that due caution ought to be exercised in the interpretation of climate model projections of extreme precipitation owing to their inadequate representation of mesoscale convective systems[21,38]. Over Sahel, where observations indicate the leading role of large mesoscale convective systems in explaining the trends in extreme precipitation[39], recent convection-permitting climate model simulations highlight tropospheric wind shear changes as the primary reason for intensifying squall lines under warming conditions[40]. Over the US, in the deep convection-driven precipitation regimes, similar tools also indicate an overwhelming role of MCS in future extreme precipitation[41]. These regional studies clearly point to the need for using new modeling approaches for global investigations as the present observational findings confirm the importance of long-lived systems to extreme precipitation over the entire tropics.

Methods

Probability of exceedance. We use two metrics to characterize precipitation distribution and the joint distribution of precipitation and MCS. First, the probability of exceedance is defined as the number of grid boxes with daily precipitation accumulation above a given threshold divided by the total number of grid boxes for the region and product under consideration. Second, the precipitation-duration joint probability of occurrence is defined as the number of grid boxes with daily precipitation accumulation above a given precipitation threshold divided by the sum of the grid boxes experiencing MCS with a duration up to the given duration weighted by its occupation of the daily grid box. The occupation is defined as the fraction of the $1° \times 1°$ occupied by an MCS during a day. The joint probability can be understood as area-weighted duration cumulated distribution of contribution to the probability of exceedance of precipitation.

Ensemble of precipitation products. A sub-ensemble of precipitation products is built from a new database of $1° \times 1° \times 1$ day gridded precipitation datasets that permits to investigate the robustness of results to the selection of the products[31]. The data used are for the 30°S–30°N region. Owing to the availability of the database of convective systems (see next section), a 5-year period spanning 2012–2016 is used for our analysis. Statistics are computed for each member of the ensemble and the resulting ensemble mean and standard deviation reported.

Twelve « flagship » products from various international groups, reflecting a large variety of estimation techniques and data sources are used initially (Table S1). Over land, the analysis of the probability of exceedance (Fig. S1 top) shows that the satellite products are relatively well clustered with very few outliers. Products mainly relying on IR are on the lower end of the probability scale for the highest daily precipitation accumulation. The most-recent version of the GPCC dataset which makes use of rain-gauge data only, exhibits the highest probability among the 12 products, over all range of precipitation. This version indeed proposes quite a different representation of the tropical precipitation from earlier versions of this product. This is likely an artifact of the update of the Kriging algorithm used[42]. Note that the land sub-ensemble product agrees well with GPCC v1 distribution. Over the ocean, the situation is similar although the spread among the cluster of products is larger than for land. The TAPR product exhibits a significant underestimation of the probability of the largest rain accumulation compared to other microwave-based products. This is likely due to the relative lack of light rain situations (Table S2).

Based on our analysis and previous studies on extreme precipitation using an ensemble of products[43], a land ensemble is built using: TAPR[44], TMPA[45], GSMArtg[46], CMORg[47], MSWE[48], and IMFC[49]. In essence, it includes all datasets using satellite microwave observations from multiple platforms (as well as IR satellite data and rain gauges except in the case of TAPR). Over ocean, the ensemble includes TMPA, GSMArtg, CMORg, MSWE, HOAP, and IMFC; thus, it is restricted to datasets using microwave observations from multiple satellites. The TAPR product is not considered over ocean, as it exhibits limited skills in depicting the tail of the precipitation distribution (Fig. S1).

The sensitivity of results to the selection of a period of 5 years is assessed using four products (TMPA, GSMArtg, CMOR, and MSWE) and comparing the probability of exceedance from 2012 to 2016 to that of a larger period, namely 2001–2016. The longer-term probability of exceedance is well within the ensemble spread (Fig. S2). This suggests that, to the precision of the ensemble spread, the probability of exceedance based on the current data selection is a good representative of that of a longer time span.

Satellite observations of mesoscale convective systems morphological characteristics. The morphology of MCS cloud shield is obtained from thermal infrared brightness temperatures measured by geostationary satellites and a detection and tracking algorithm as done classically[50,51]. Here we use the Tracking Of Organized Convection Algorithm through a 3D segmentatioN (TOOCAN) algorithm[33]. Previous techniques, based on overlap statistics, are prone to artificially extend the duration of MCS owing to some split and merge artifacts. An issue that the TOOCAN approach has overcome[33]. This algorithm first performs a multi-threshold multi-step screening on the space and time infrared image volume to detect convective seeds. Then, it grows them towards the edges of their stratiform extension (defined by a 235 K threshold), as done in previous studies. The outputs of the algorithm are various morphological parameters of the cold cloud shield (geolocation, size, brightness temperature distribution) as a function of the MCS life cycle, with a temporal resolution of 30 minutes. From these raw outputs, many integrated MCS parameters are built: duration, distance of propagation, average speed of propagation, etc. In this study we focus on the duration parameter.

Earlier versions of this MCS database have been derived from various geostationary archives, and used in a number of studies to investigate the contribution of MCS to the distribution of tropical rainfall[13], the radiative properties of the MCS[52], their life cycle behavior[22] and intraseasonal variability[53]. Here, the algorithm is applied to a recently developed homogenized multi geostationary infrared imagery archive covering all of tropics for the period 2012–2016[54], thus providing the best estimate to date of the MCS distribution in the tropics.

The quality control of the MCS dataset is stringent. The tracking algorithm indeed nominally requires 30-min image sampling. During the MTSAT-1 and 2 operations (from 2012 to May 2015) over the Western Pacific, the acquisition scheme only provids northern hemisphere imagery at a 30-minute rate; the full hemisphere images were available only once every hour. As a result, no tracking is performed for the southern hemisphere between 100 W and 100E. After June 2015 and the shift to HIMAWARI-8, the required temporal sampling is available for both hemispheres and MCS statistics are computed accordingly. The two GOES satellites have a complex acquisition scheme whereby the high-frequency full images scans are often disrupted due to operational survey of hurricanes. Consequently, after compositing all available imagery, a narrow band between 116 °W and 105 °W and 0 °S and 30 °S is left unobserved with the required 30-minute sampling rate, for which no MCS statistics are available. In complement to the nominal functioning and the above-mentioned limitations, it happens that some periods of time are operated under degraded quality and services. The tracking algorithm, through interpolation, can handle exceptionally, short interruptions of up to 2 h 30 min. Beyond that 2 h 30 min threshold, MCS are all terminated and new systems are considered to have been born, causing an unphysical bias in the duration statistics. In order to avoid such artifacts, only those days with all images available have been retained in our analysis. This results in less availability than the precipitation datasets. For each product, this sub-sampling corresponds to ~75% of the original valid precipitation data. The effect of sub-sampling on the distribution of extreme precipitation is either within (up to ~100 mm/d) or much

smaller (for precipitation above ~100 mm/d) than the ensemble spread (Fig. S2). The filtering of precipitation products on the sampling of the MCS database does not impact our results.

The morphological parameters of convective systems have been gridded on the same 1° × 1° daily grid as the precipitation estimates, so as to enable simultaneous analysis of storm characteristics and precipitation amount. In this Eulerian framework, the properties of systems are viewed from a grid box perspective. The method was introduced and used in the past[13,53]. The full resolution cold pixels from geostationary observations are projected on a 1° × 1° daily grid for each cluster composing each system. The cold cloudiness occupation of a grid box and the morphological properties of each system are then assigned to that grid box. If a system cluster is large enough and/or is located as to cover more than one grid box at a time, the cold cloudiness of this system is hence distributed onto each of the associated grid boxes. Similarly, when a system is lasting more than a day, the associated cold cloudiness is distributed over all relevant days. Owing to the propagation, size, and arrangements, multiple systems can be observed over a given 1° × 1° grid box during any day, and can all contribute to the total cold cloudiness of that particular grid box. While the joint distribution of MCS occurrence with precipitation at the 1° × 1° scale indicates that each grid box can see cloud cover contributions from up to 25 individual systems in a day, only a couple of MCS are indeed significantly impacting each grid box while most of the other systems have very small contributions to the cold cloudiness as illustrated in Fig. S3. In the joint statistics presented here, the morphological properties of systems are weighted using the actual cold cloudiness of each system in each grid box.

Data availability

The precipitation datasets analyzed during the current study are identified under the https://doi.org/10.14768/06337394-73A9-407C-9997-0E380DAC5598 and are available at http://frogs.ipsl.fr. The MSWEP data were acquired directly from H. Beck and are available at http://www.gloh2o.org/. The MCS database is identified under the https://doi.org/10.14768/20191112002.1 and is available at http://toocan.ipsl.fr.

Received: 2 March 2020; Accepted: 11 August 2020;
Published online: 14 September 2020

References

1. Roca, R. et al. On the water and energy cycles in the Tropics. *Comptes Rendus - Geosci.* **342**, 390–402 (2010).
2. Ramanathan, V. The role of ocean-atmosphere interactions in the CO2 climate problem. *J. Atmosph. Sci.* **38**, 918–930 (1981).
3. Stephens, G. L. & Ellis, T. D. Controls of global-mean precipitation increases in global warming GCM experiments. *J. Clim.* **21**, 6141–6155 (2008).
4. Trenberth, K. E. Changes in precipitation with climate change. *Clim. Res.* **47**, 123–138 (2011).
5. O'Gorman, P. A. & Schneider, T. The physical basis for increases in precipitation extremes in simulations of 21st-century climate change. *Proc. Natl. Acad. Sci. USA* **106**, 14773–14777 (2009).
6. Fischer, E. M. & Knutti, R. Observed heavy precipitation increase confirms theory and early models. *Nat. Clim. Chang.* **6**, 986–991 (2016).
7. O'Gorman, P. A. Precipitation extremes under climate change. *Curr. Clim. Chang. Reports* **1**, 49–59 (2015).
8. Westra, S. et al. Future changes to the intensity and frequencyof short-duration extreme rainfall. *Rev. Geophys.* **52**, 522–555 (2014).
9. Roca, R. Estimation of extreme daily precipitation thermodynamic scaling using gridded satellite precipitation products over tropical land. *Environ. Res. Lett.* https://doi.org/10.1088/1748-9326/ab35c6 (2019).
10. Muller, C. J. & Takayabu, Y. Response of precipitation extremes to warming: what have we learned from theory and idealized cloud-resolving simulations, and what remains to be learned? *Environ. Res. Lett.* https://doi.org/10.1088/1748-9326/ab7130 (2020).
11. Houze, R. A. Mesoscale convective systems. *Rev. Geophys.* **42**, 1–43 (2004).
12. Liu, C. Rainfall contributions from precipitation systems with different sizes, convective intensities, and durations over the tropics and subtropics. *J. Hydrometeorol.* **12**, 394–412 (2011).
13. Roca, R., Aublanc, J., Chambon, P., Fiolleau, T. & Viltard, N. Robust observational quantification of the contribution of mesoscale convective systems to rainfall in the tropics. *J. Clim.* **27**, 4952–4958 (2014).
14. Houze, R. A. 100 years of research on MCS. *Am. Meteorol. Soc. Monogr.* https://doi.org/10.1175/AMSMONOGRAPHS-D-18-0001.1 (2018).
15. Ahmed, F. & Schumacher, C. Convective and stratiform components of the precipitation-moisture relationship. *Geophys. Res. Lett.* **42**, 10453–10462 (2015).
16. Holloway, C. E. et al. Observing convective aggregation. In: *Surveys in Geophysics* vol. 38 (Springer Netherlands, 2017).
17. Semie, A. G. & Bony, S. Relationship between precipitation extremes and convective organization inferred from satellite observations. *Geophys. Res. Lett.* **47**, e2019GL086927 https://doi.org/10.1029/2019GL086927 (2020).
18. Bao, J., Sherwood, S. C., Colin, M. & Dixit, V. The robust relationship between extreme precipitation and convective organization in idealized numerical modeling simulations. *J. Adv. Model. Earth Syst.* **9**, 2291–2303 (2017).
19. Lee, D., Oreopoulos, L., Huffman, G. J., Rossow, W. B. & Kang, I. S. The precipitation characteristics of isccp tropical weather states. *J. Clim.* **26**, 772–788 (2013).
20. Tan, J., Jakob, C., Rossow, W. B. & Tselioudis, G. Increases in tropical rainfall driven by changes in frequency of organized deep convection. *Nature* **519**, 451–454 (2015).
21. Rossow, W. B., Mekonnen, A., Pearl, C. & Goncalves, W. Tropical precipitation extremes. *J. Clim.* **26**, 1457–1466 (2013).
22. Roca, R., Fiolleau, T. & Bouniol, D. A simple model of the life cycle of mesoscale convective systems cloud shield in the tropics. *J. Clim.* **30**, 4283–4298 (2017).
23. Liu, C. & Zipser, E. J. The global distribution of largest, deepest, and most intense precipitation systems. *Geophys. Res. Lett.* **42**, 3591–3595 (2015).
24. Hamada, A., Takayabu, Y. N., Liu, C. & Zipser, E. J. Weak linkage between the heaviest rainfall and tallest storms. *Nat. Commun.* **6**, 6213 (2015).
25. Hamada, A. & Takayabu, Y. N. Large-scale environmental conditions related to midsummer extreme rainfall events around Japan in the TRMM region. *J. Clim.* **31**, 6933–6945 (2018).
26. Romatschke, U. & Houze, R. A. Extreme summer convection in South America. *J. Clim.* **23**, 3761–3791 (2010).
27. Taylor, C. M. et al. Frequency of extreme Sahelian storms tripled since 1982 in satellite observations. *Nature* **544**, 475–478 (2017).
28. Feng, Z. et al. More frequent intense and long-lived storms dominate the springtime trend in central US rainfall. *Nat. Commun.* **7**, 1–8 (2016).
29. Muller, C. J., O'Gorman, P. A. & Back, L. E. Intensification of precipitation extremes with warming in a cloud-resolving model. *J. Clim.* **24**, 2784–2800 (2011).
30. Singleton, A. & Toumi, R. Super-Clausius-Clapeyron scaling of rainfall in a model squall line. *Q. J. R. Meteorol. Soc.* **139**, 334–339 (2013).
31. Roca, R. et al. FROGS: a daily 1° × 1° gridded precipitation database of rain gauge, satellite and reanalysis products. *Earth Syst. Sci. Data.* **11**, 1017–1035 (2019).
32. Alexander, L. V. et al. Intercomparison of annual precipitation indices and extremes over global land areas from in situ, space-based and reanalysis products. *Environ. Res. Lett.* **15**, (2020).
33. Fiolleau, T. & Roca, R. An algorithm for the detection and tracking of tropical mesoscale convective systems using infrared images from geostationary satellite. *IEEE Trans. Geosci. Remote Sens.* **51**, 4302–4315 (2013).
34. Roca, R., Bouniol, D. & Fiolleau, T. On the duration and life cycle of precipitation systems in the tropics. In: (eds Levizzani, V. et al.), Satellite Precipitation Measurement, Springer Nature, Cham. *Advances in Global Change Research* **69**, 729–744 (2020).
35. Liu, C. Rainfall contributions from precipitation systems with different sizes, convective intensities, and durations over the tropics and subtropics. *J. Hydrometeorol* **12**, 394–412 (2011).
36. Vant-Hull, B., Rossow, W. & Pearl, C. Global comparisons of regional life cycle properties and motion of multiday convective systems: tropical and midlatitude land and ocean. *J. Clim.* **29**, 5837–5858 (2016).
37. Heikenfeld, M. et al. Tobac V1.0: towards a flexible framework for tracking and analysis of clouds in diverse datasets. *Geosci. Model Dev. Discuss* **20**, 1–31 (2019).
38. Prein, A. F. et al. A review on regional convection-permitting climate modeling: demonstrations, prospects, and challenges. *Rev. Geophys.* **53**, 323–361 (2015).
39. Taylor, C. M. et al. Frequency of extreme Sahelian storms tripled since 1982 in satellite observations. *Nature* **544**, 475–478 (2017).
40. Fitzpatrick, R. G. J. et al. What drives the intensification of mesoscale convective systems over the West African Sahel under climate change? *J. Clim.* **33**, 3151–3172 (2020).
41. Prein, A. F. et al. Increased rainfall volume from future convective storms in the US. *Nat. Clim. Chang.* **7**, 880–884 (2017).
42. Alexander, L. V. et al. Intercomparison of annual precipitation indices and extremes over global land areas from in situ, space-based and reanalysis products. *Environ. Res. Lett.* **15**, 055002 (2020).
43. Masunaga, H. et al. Inter-product biases in global precipitation extremes. *Environ. Res. Lett.* **14**, 125016 (2019).
44. Roca, R. et al. Quantifying the contribution of the Megha-Tropiques mission to the estimation of daily accumulated rainfall in the Tropics. *Q J R Meteorol Soc* **144**, 49–63 (2018).
45. Huffman, G. J., Adler, R. F., Bolvin, D. T. & Nelkin, E. J. The TRMM multi-satellite precipitation analysis (TMPA). In: (eds Surface, H., Ferdous, H.,

Gebremichael, M. & Verlag.), *Satellite Rainfall Applications for Surface Hydrology* https://doi.org/10.1007/978-90-481-2915-7_1. (2009).
46. Kubota, T. et al. Global precipitation map using satellite-borne microwave radiometers by the GSMaP project: production and validation. *IEEE Trans. Geosci. Remote Sens.* **45**, 2259–2275 (2007).
47. Xie, P. et al. Reprocessed, bias-corrected CMORPH global high-resolution precipitation estimates from 1998. *J. Hydrometeorol.* **18**, 1617–1641 (2017).
48. Beck, H. E. et al. MSWep v2 Global 3-hourly 0.1° precipitation: methodology and quantitative assessment. *Bull. Am. Meteorol. Soc* **100**, 473–500 (2019).
49. Huffman, G. J. et al. NASA Global Precipitation Measurement (GPM) Integrated Multi-satellitE Retrievals for GPM (IMERG). *Algorithm Theor. Basis Doc.* https://pmm.nasa.gov/resources/documents/gpm-integrated-multi-satellite-retrievals-gpm-imerg-algorithm-theoretical-basis- (2018).
50. Williams, M. & Houze, R. A. Satellite-observed characteristics of winter monsoon cloud clusters. *Mon. Weather Rev.* **115**, 505–519 (1987).
51. Toledo Machado, L. A., Desbois, M. & Duvel, J. P. Structural characteristics of deep convective systems over tropical Africa and the Atlantic Ocean. *Mon. Weather Rev.* **120**, 392–406 (1992).
52. Bouniol, D., Roca, R., Fiolleau, T. & Poan, D. E. Macrophysical, microphysical and radiative properties of tropical Mesocale Convective Systems over their life cycle. *J. Clim.* https://doi.org/10.1175/JCLI-D-15-0551.1 (2016).
53. Berthet, S., Roca, R., Duvel, J. P. & Fiolleau, T. Subseasonal variability of mesoscale convective systems over the tropical northeastern Pacific. *Q. J. R. Meteorol. Soc.* **143**, 1086–1094 (2017).
54. Fiolleau, T., Roca, R., Cloche, S., Bouniol, D. & Raberanto, P. Homogenization of geostationary infrared imager channels for cold cloud studies using megha-tropiques/ScaRaB. *IEEE Trans. Geosci. Remote Sens.* https://doi.org/10.1109/tgrs.2020.2978171 (2020).

Acknowledgements

We thank S. Cloché for her help with the handling of the multiple datasets used here. This study benefited from the IPSL mesocenter ESPRI facility, which is supported by CNRS, UPMC, Labex L-IPSL, CNES, and Ecole Polytechnique. This study was supported by CNES and CNRS under the Megha-Tropiques program.

Author contributions

R.R. initiated the study and performed the analysis. T.F. developed and adapted the TOOCAN algorithm to the recent observations and commissioned the cloud tracking dataset. Both authors discussed the results and edited the manuscript.

Competing interests

The authors declare no competing interests.

Additional information

Supplementary information is available for this paper at https://doi.org/10.1038/s43247-020-00015-4.

Correspondence and requests for materials should be addressed to R.R.

Peer review information Primary handling editors: Heike Langenberg

Reprints and permission information is available at http://www.nature.com/reprints

Publisher's note Springer Nature remains neutral with regard to jurisdictional claims in published maps and institutional affiliations.

Open Access This article is licensed under a Creative Commons Attribution 4.0 International License, which permits use, sharing, adaptation, distribution and reproduction in any medium or format, as long as you give appropriate credit to the original author(s) and the source, provide a link to the Creative Commons license, and indicate if changes were made. The images or other third party material in this article are included in the article's Creative Commons license, unless indicated otherwise in a credit line to the material. If material is not included in the article's Creative Commons license and your intended use is not permitted by statutory regulation or exceeds the permitted use, you will need to obtain permission directly from the copyright holder. To view a copy of this license, visit http://creativecommons.org/licenses/by/4.0/.

© The Author(s) 2020